A level set algorithm for minimizing the Mumford-Shah functional in image processing*

Tony F. Chan
Department of Mathematics
University of California, Los Angeles
Los Angeles, CA 90095-1555
chan@math.ucla.edu

Luminita A. Vese
lvese@math.ucla.edu

Abstract

We show how the piecewise-smooth Mumford-Shah segmentation problem [25] can be solved using the level set method of S. Osher and J. Sethian [26]. The obtained algorithm can be simultaneously used to denoise, segment, detect-extract edges, and perform active contours. The proposed model is also a generalization of a previous active contour model without edges, proposed by the authors in [12], and of its extension to the case with more than two segments for piecewise-constant segmentation [11]. Based on the Four Color Theorem, we can assume that in general, at most two level set functions are sufficient to detect and represent distinct objects of distinct intensities, with triple junctions, or T-junctions.

1. Introduction

In this paper, we propose a multi-phase level set formulation and algorithm for the general Mumford-Shah minimization problem [25] in image processing, to compute piecewise-smooth optimal approximations of a given image. The proposed model follows and fully generalizes our previous related works: in [12], we have proposed an active contour model without edges based on a 2-phase segmentation and level sets; in [10], we have extended the model from [12] to vector-valued images; and finally, in [11], we have extended the model from [12] to piecewise-constant segmentation of images, allowing for more then two segments, triple junctions and complex topologies, using a new multi-phase level set formulation and partition of the image-domain.

In this paper, we further generalize these previous works to the piecewise-smooth Mumford-Shah model, in several directions:

1) In one dimension: for signal segmentation and denoising, we show that, using only one level set function, we can represent any signal with any number of segments in the partition.

2) In two dimensions:

(i) we generalize the 2-phase piecewise-constant model from [12] to piecewise-smooth optimal approximations using only one level set function: different regions of distinct intensities can be represented and detected.

(ii) following the idea of the multi-phase level set partition from [11], we show that, in the piecewise-smooth case, using only two level set functions, producing up to four phases, any general case can be considered and represented by the proposed formulation. Our main idea is based on the Four Color Theorem.

We think that the proposed level set formulations and results based on the Mumford-Shah model [25] are new. We would only like to mention that ideas very similar with those from part 2(i) above have been also developed by A. Tsai, A. Yezzi, and A. Willsky in several works (such as [33]), independently and contemporaneously, again as a generalization of the model from [12].

Let $\Omega \subset \boldsymbol{R}^N$ ($N \geq 1$), be open and bounded, and let $u_0 : \Omega \to \boldsymbol{R}$ be a bounded function, representing the initial image (here, for simplicity, we restraint our discussion to single-valued functions u, but the vector-valued case could be considered in a similar way). Later, we will consider only the cases $N = 1$ (signals) and $N = 2$ (images).

Let $\Gamma \subset \Omega$ be a closed subset, made up of a finite set of smooth hyper-surfaces.

To solve the segmentation problem, D. Mumford and J. Shah proposed the following minimization problem [25], written here in any dimension N:

$$\inf_{u,\Gamma} \left\{ F^{MS}(u, \Gamma) \right. \tag{1}$$

*This work has been supported in part by ONR Contract N00014-96-1-0277 and NSF Contract DMS-9973341.

0-7695-1278-X/01 $10.00 © 2001 IEEE

$$= \int_\Omega |u-u_0|^2 dx + \mu \int_{\Omega\setminus\Gamma} |\nabla u|^2 dx + \nu \mathcal{H}^{N-1}(\Gamma)\Big\},$$

where $\mathcal{H}^{N-1}(\Gamma)$ stands for the $(N-1)$-dimensional Hausdorf measure, and $\mu > 0$, $\nu > 0$ are fixed parameters, to weight the different terms in the energy. A minimizer of the above energy will be an "optimal" piecewise-smooth approximation of the initial, possible noisy, image u_0; Γ has the role of approximating the edges in the image u_0, and u will be smooth only outside Γ, i.e. on $\Omega \setminus \Gamma$.

It is not easy to minimize in practice the functional (1), because of the unknown set Γ of lower dimension, and also because the problem is not convex.

A weak formulation of (1) has been proposed by G. Dal Maso, J.M. Morel and S. Solimini in [14], where Γ is replaced by the set J_u of jumps of u, in order to prove the existence of minimizers. It is known that a global minimizer of (1), or of the weak formulation, is not unique in general. In [22] and [23], the authors proposed a constructive existence result in the piecewise-constant case, and in [20], a practical algorithm based on regions growing and merging is proposed for this case. For a general exposition of the segmentation problem by variational methods, both in theory and practice, we refer the reader to [24].

L. Ambrosio and V.M. Tortorelli proposed two elliptic approximations by Γ-convergence to the weak formulation of the Mumford-Shah functional in [2] and [3]. They approximated a minimizer (u, J_u) of $F^{MS}(u, J_u)$, by two smooth functions (u_ρ, v_ρ), such that, as $\rho \to 0$, $u_\rho \to u$ and $v_\rho \to 1$ in the $L^2(\Omega)$-topology, and v_ρ is different from 1 only in a small neighborhood of J_u, which shrinks as $\rho \to 0$. The elliptic approximations lead to a coupled system of two equations in the unknowns u_ρ and v_ρ, to which standard PDE methods can be applied (see [21], [7], [8], [5], [4]). In [9], A. Chambolle and G. Dal Maso provide an approximation by $\Gamma - convergence$ based on the finite element method.

Finally, we would like to refer the reader to other related works on segmentation, such as: [27], [36], [34], [33], [31], [29] and [30], [28], to a variational level set approach to multiphase motion [35], and also to [15].

The outline of the paper is as follows. In subsection 2.1, we consider the one-dimensional case of signal segmentation; we show here that using only one level set function, any signal can be represented, with any number of segments in the partition. In subsection 2.2, we consider the two-dimensional case, showing that, using one level set function and the piecewise-smooth Mumford-Shah energy, we can represent, detect and denoise different objects of different intensities (not necessarily constant). In subsection 2.3, by considering only one more level set function, based on the Four Color Theorem, we propose a new multi-phase level set formulation to the general piecewise-smooth Mumford-Shah model, without restriction on the type of edges in the image. Each time, we show experimental results on synthetic and real images, by the proposed models. Finally, we end the paper by a short concluding section.

2. Piecewise-smooth Mumford-Shah segmentation by level sets

We describe in this section the proposed models, and we show experimental results in each case. Let us first give some of the main notations.

The Heaviside function H in one dimension is defined by:

$$H(z) = \begin{cases} 1, \text{ if } z \geq 0, \\ 0, \text{ if } z < 0. \end{cases}$$

We will also use smooth regularizations and approximations $H_\varepsilon \in C^1(\mathbf{R})$ of H, as $\varepsilon \to 0$, and we will use the notation $\delta_\varepsilon = H'_\varepsilon$ (see [12] for examples of such approximations).

Following the level set method, introduced by S. Osher and J. Sethian [26], we will denote by $\phi : \Omega \to \mathbf{R}$ a Lipschitz function, called level set function, such that, when $\Gamma = \partial\omega$, with $\omega \subset \Omega$ open and bounded, then $\phi(x) = 0$ on Γ, $\phi(x) > 0$ if $x \in \omega$, and $\phi(x) < 0$ if $x \in \Omega \setminus \omega$. In this case, a hypersurface Γ is represented by the zero level set of ϕ. This formulation has many computational advantages for evolution of fronts and tracking interfaces: it allows for a fixed rectangular grid, and merging and breaking of the evolving hypersurface are done automatically.

We recall that we have the following formula [16]: $\mathcal{H}^{N-1}(\Gamma) = \int_\Omega |\nabla H(\phi)|$, the integral being in the sense of measures, and this gives the cardinal of Γ in dimension one, the length of Γ in two dimensions, etc.

The main contribution of this paper is to propose a level set formulation and algorithm for minimizing the Mumford-Shah energy, in the strong formulation (1), in the general case, with at most two level set functions, representing the set of edges in the image. As we have mentioned, there are many works for the weak formulation, but not for the strong formulation.

We also follow techniques and terminology from a related work on a variational level set approach to multiphase motion [35].

2.1. The one-dimensional case: signal denoising and segmentation

For $N = 1$ and $x \in \mathbf{R}$, we deal with a source signal u on $\Omega = (a, b)$. The problem of reconstructing u from a disturbed input u_0 deriving from a distorted transmission, can be modeled as finding the minimum

$$\min_{u,\Gamma} \Big\{ \mu \int_{(a,b)\setminus\Gamma} |u'|^2 dx + \int_a^b |u-u_0|^2 dx + \nu \#(\Gamma) \Big\}, \quad (2)$$

where Γ denotes in fact the set of discontinuity points of u, and $\#(\Gamma) = \mathcal{H}^0(\Gamma)$ denotes the cardinal of Γ.

We let $\Gamma = \Big\{x \in (a,b) |\ \phi(x) = 0\Big\}$, and we introduce two functions u^+ and u^-, such that

$$u(x) = u^+(x)H\Big(\phi(x)\Big) + u^-(x)\Big(1 - H\Big(\phi(x)\Big)\Big).$$

These two functions replace the two unknown constants used in [12], and are such that $u^+ \in C^1(\{\phi \geq 0\})$, and $u^- \in C^1(\{\phi \leq 0\})$. Then the energy (2) can be written in the level set formulation as:

$$\min_{u^+,u^-,\phi} \Big\{\mu \int_a^b |(u^+)'|^2 H(\phi)dx + \mu \int_a^b |(u^-)'|^2(1 - H(\phi))dx + \int_a^b |u^+ - u_0|^2 H(\phi)dx + \int_a^b |u^- - u_0|^2(1 - H(\phi))dx + \nu \int_a^b |H(\phi)'|.\Big\}$$

Minimizing this energy with respect to u^+, u^-, and ϕ, and regularizing the Heaviside function H, we obtain the associated Euler-Lagrange equations:

$$u^+ - u_0 = \mu(u^+)'' \text{ in } \{\phi > 0\},\ (u^+)' = 0 \text{ if } \phi = 0,$$
$$u^- - u_0 = \mu(u^-)'' \text{ in } \{\phi < 0\},\ (u^-)' = 0 \text{ if } \phi = 0,$$
$$\frac{\partial \phi}{\partial t} = \delta_\varepsilon(\phi)\Big[\nu\Big(\frac{\phi'}{|\phi'|}\Big)' - |u^+ - u_0|^2 + |u^- - u_0|^2 - \mu|(u^+)'|^2 + \mu|(u^-)'|^2\Big].$$

We will discuss in the end of the paper the main steps of the numerical algorithm for solving the above Euler-Lagrange equations.

We remark that, in one dimension for signal segmentation, only one level set function suffices to represent a piecewise-smooth function u together with its set of jumps.

We end this subsection by an experimental result for signal denoising and segmentation. We show in Figure 1 an original and noisy signal, together with two points, where $\phi = 0$ initially. In Figure 2, we show the segmented signal, and the detected set of jumps given by $\phi = 0$ at the steady state, using the proposed level set algorithm. Note that piecewise-smooth regions are very well reconstructed by the model, and that the jumps are well located and without smearing.

2.2. The two-dimensional case: two-phase model

In this subsection, we consider the two-dimensional case ($N = 2$ and $x \in \mathbb{R}^2$), under the assumption that the edges

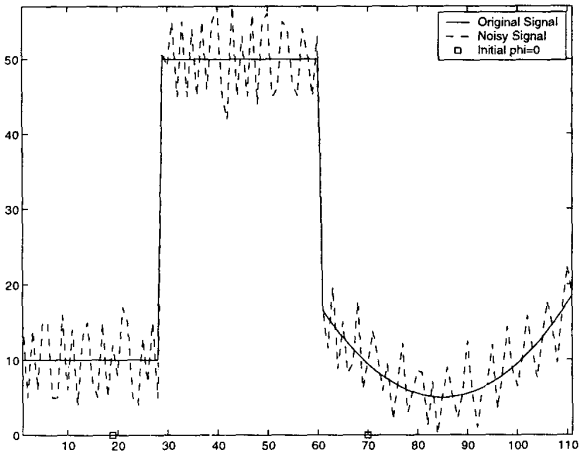

Figure 1. Original and noisy signal, together with the set of points where $\phi = 0$ initially, represented by squares on the x–axis.

(denoted by Γ) in the image can be represented by one level set function. The general case, allowing for any type of edges, including triple junctions, will be considered in the next subsection.

As in the 1-dimensional case, the link between the unknowns u and ϕ can be expressed by introducing two functions u^+ and u^-, such that

$$u(x) = \begin{cases} u^+(x) \text{ if } \phi(x) \geq 0, \\ u^-(x) \text{ if } \phi(x) < 0. \end{cases}$$

We assume that u^+ and u^- are C^1 functions on $\phi \geq 0$ and on $\phi \leq 0$ respectively (and therefore with continuous derivatives up to all boundary points, i.e. up to the boundary $\{\phi = 0\}$). We illustrate our formulation in Figure 3.

Then we obtain the following minimization problem from (1):

$$\inf_{u^+,u^-,\phi} F(u^+, u^-, \phi),$$

where

$$F(u^+, u^-, \phi) = \int_\Omega |u^+ - u_0|^2 H(\phi)dx + \int_\Omega |u^- - u_0|^2(1 - H(\phi))dx + \mu \int_\Omega |\nabla u^+|^2 H(\phi))dx + \mu \int_\Omega |\nabla u^-|^2(1 - H(\phi))dx + \nu \int_\Omega |\nabla H(\phi)|.$$

Keeping first ϕ fixed and minimizing $F(u^+, u^-, \phi)$ with respect to u^+ and u^-, we obtain the following Euler-Lagrange equations for u^+ and u^-:

$$u^+ - u_0 = \mu \Delta u^+ \text{ on } \phi > 0,\ \frac{\partial u^+}{\partial \vec{n}} = 0 \text{ on } \{\phi = 0\}, \quad (3)$$

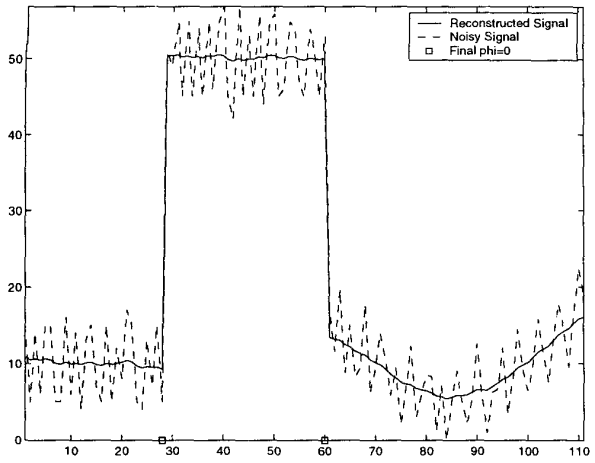

Figure 2. Segmentation of the noisy signal: reconstructed signal, noisy signal, and the set of points where $\phi = 0$ at the steady state.

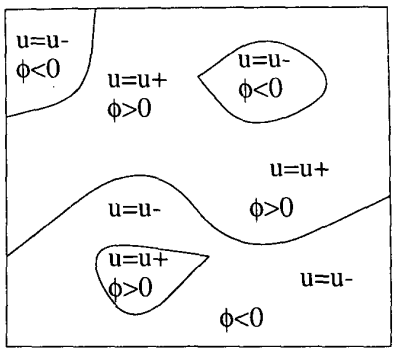

Figure 3. Example of partition of the image u in regions, with boundaries Γ represented via a single level set function ($\phi = 0$), and with smooth value-functions u^+ and u^- on each side of the curve.

$$u^- - u_0 = \mu \triangle u^- \text{ on } \phi < 0, \ \frac{\partial u^-}{\partial \vec{n}} = 0 \text{ on } \{\phi = 0\}, \quad (4)$$

where $\partial / \partial \vec{n}$ denotes the partial derivative in the normal direction $\vec{n}$ at the boundary $\{\phi = 0\}$. These two equations will have a smoothing and denoising effect on the image u_0, but only inside homogeneous regions, and not across edges.

Now, keeping the functions u^+ and u^- fixed, and minimizing $F(u^+, u^-, \phi)$ with respect to ϕ, we obtain the following Euler-Lagrange equation along the curve $\{\phi = 0\}$:

$$\frac{\partial \phi}{\partial t} = \delta_\varepsilon(\phi)\Big[\nu \nabla\Big(\frac{\nabla \phi}{|\nabla \phi|}\Big) - |u^+ - u_0|^2 \quad (5)$$
$$-\mu |\nabla u^+|^2 + |u^- - u_0|^2 + \mu |\nabla u^-|^2\Big].$$

Again, we will discuss in the end of the paper the main steps of the numerical algorithm, in order to solve the above Euler-Lagrange equations.

We show in Figures 4 and 5 two numerical results using the proposed algorithm: each time, the evolving curves are superposed over the initial noisy image u_0 (top), and the denoised versions u of u_0 are also shown (bottom), at different increasing times. In Figure 4, we see that the model performs as active contours, denoising and edge-detection. In Figure 5, we apply the model to a real piecewise-smooth image.

2.3. The two-dimensional case: four-phase model

In the previous subsection, we have shown how we can minimize the general Mumford-Shah functional for segmentation in the case where the set of contours Γ can be represented by a single level set function, i.e. $\Gamma = \{\phi = 0\}$ and ϕ has opposite signs on each side of Γ. By this method, we can already detect several objects of distinct gray-levels, but we have a constraint on the type of edges. There are cases where the boundaries of regions forming a partition of the image could not be represented in this way (i.e. using a single level set function). Again, the natural idea is to use more than one level set function, as in [11] for the piecewise-constant case with more than two segments.

We show that in the general case, the problem can be solved using only two level set functions, and we do not have to know a-priori how many gray-levels the image has (or how many segments). The idea is based on the Four Color Theorem and is as follows.

Based on this observation, we can "color" all the regions in a partition using only four "colors", such that any two adjacent regions have different "colors". Therefore, using two level set functions, we can identify the four "colors" by the following (disjoint) sets: $\{\phi_1 > 0, \ \phi_2 > 0\}$, $\{\phi_1 < 0, \ \phi_2 < 0\}$, $\{\phi_1 < 0, \ \phi_2 > 0\}$, $\{\phi_1 < 0, \ \phi_2 < 0\}$. The boundaries of the regions forming the partition will be given by $\{\phi_1 = 0\} \cup \{\phi_2 = 0\}$, and this will be the set of curves Γ. Note that, in our particular multiphase formulation of the problem, we do not have the problems of "overlapping" or "vacuum", (i.e. the phases are disjoint, and their union is the entire domain Ω). This is an improvement over the multi-phase formulations used in [35] and [28], where the authors needed to add additional constraints to reinforce the partition. Moreover, as we have already shown in [11], triple junctions can be represented using only two level set functions.

As in the previous subsection, the link between the func-

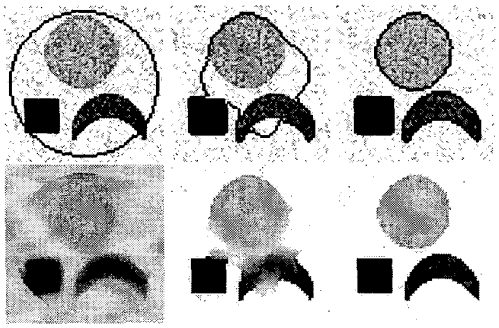

Figure 4. Results on a noisy image, using our level set algorithm for the Mumford-Shah model. The algorithm performs as an active contour model, denoising and edge detection.

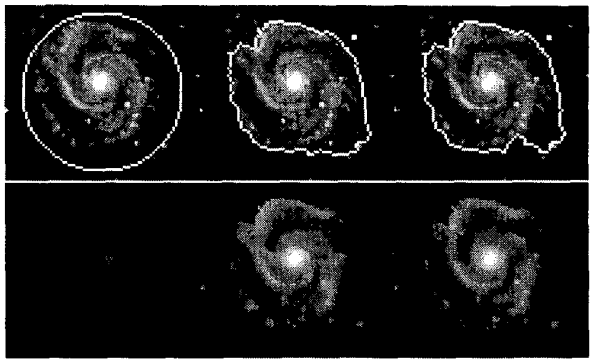

Figure 5. Numerical results on a real image, using the proposed level set algorithm with one level set function.

tion u and the four regions can be made by introducing four functions $u^{++}, u^{+-}, u^{-+}, u^{--}$, which are in fact the restrictions of u to each of the four phases, as follows:

$$u(x) = \begin{cases} u^{++}(x), \text{ if } \phi_1(x) > 0 \text{ and } \phi_2(x) > 0, \\ u^{+-}(x), \text{ if } \phi_1(x) > 0 \text{ and } \phi_2(x) < 0, \\ u^{-+}(x), \text{ if } \phi_1(x) < 0 \text{ and } \phi_2(x) > 0, \\ u^{--}(x), \text{ if } \phi_1(x) < 0 \text{ and } \phi_2(x) < 0. \end{cases}$$

These notations are illustrated in Figure 6.

Again, using the Heaviside function, the relation between u, the four functions u^{++}, u^{+-}, u^{-+}, u^{--}, and the level set functions ϕ_1 and ϕ_2 can be expressed by a single relation:

$u = u^{++}H(\phi_1)H(\phi_2) + u^{+-}H(\phi_1)(1 - H(\phi_2)) + u^{-+}(1 - H(\phi_1))H(\phi_2) + u^{--}(1 - H(\phi_1))(1 - H(\phi_2))$.

Using the notation $\Phi = (\phi_1, \phi_2)$, we introduce an energy in level set formulation, based on the Mumford-Shah functional (1):

$$\begin{aligned} F(u, \Phi) = &\int_\Omega |u^{++} - u_0|^2 H(\phi_1)H(\phi_2)dx \\ &+\mu \int_\Omega |\nabla u^{++}|^2 H(\phi_1)H(\phi_2)dx \\ &+ \int_\Omega |u^{+-} - u_0|^2 H(\phi_1)(1 - H(\phi_2))dx \\ &+\mu \int_\Omega |\nabla u^{+-}|^2 H(\phi_1)(1 - H(\phi_2))dx \\ &+ \int_\Omega |u^{-+} - u_0|^2 (1 - H(\phi_1))H(\phi_2)dx \\ &+\mu \int_\Omega |\nabla u^{-+}|^2 (1 - H(\phi_1))H(\phi_2)dx \\ &+ \int_\Omega |u^{--} - u_0|^2 (1 - H(\phi_1))(1 - H(\phi_2))dx \\ &+\mu \int_\Omega |\nabla u^{--}|^2 (1 - H(\phi_1))(1 - H(\phi_2))dx \\ &+\nu \int_\Omega |\nabla H(\phi_1)| + \nu \int_\Omega |\nabla H(\phi_2)|. \end{aligned}$$

Note that, the expression $\int_\Omega |\nabla H(\phi_1)| + \int_\Omega |\nabla H(\phi_2)|$ is not exactly the length term, it is just an approximation and simplification. By this approximation formula, in some cases, some parts of the curves may count more than once. In practice, we have obtained satisfactory results using the above formula, and the associated Euler-Lagrange equations are simplified.

We obtain the associated Euler-Lagrange equations as in the previous case. If ϕ_1 and ϕ_2 are fixed, minimizing the energy with respect to the functions u^{++}, u^{+-}, u^{-+}, u^{--}, we obtain:

$$\begin{aligned} u^{++} - u_0 &= \mu \Delta u^{++} \text{ in } \{\phi_1 > 0, \phi_2 > 0\}, \\ \frac{\partial u^{++}}{\partial \vec{n}} &= 0 \text{ on } \{\phi_1 = 0, \phi_2 \geq 0\}, \{\phi_1 \geq 0, \phi_2 = 0\}; \\ u^{+-} - u_0 &= \mu \Delta u^{+-} \text{ in } \{\phi_1 > 0, \phi_2 < 0\}, \\ \frac{\partial u^{+-}}{\partial \vec{n}} &= 0 \text{ on } \{\phi_1 = 0, \phi_2 \leq 0\}, \{\phi_1 \geq 0, \phi_2 = 0\}; \\ u^{-+} - u_0 &= \mu \Delta u^{-+} \text{ in } \{\phi_1 < 0, \phi_2 > 0\}, \\ \frac{\partial u^{-+}}{\partial \vec{n}} &= 0 \text{ on } \{\phi_1 = 0, \phi_2 \geq 0\}, \{\phi_1 \leq 0, \phi_2 = 0\}; \\ u^{--} - u_0 &= \mu \Delta u^{--} \text{ in } \{\phi_1 < 0, \phi_2 < 0\}, \\ \frac{\partial u^{--}}{\partial \vec{n}} &= 0 \text{ on } \{\phi_1 = 0, \phi_2 \leq 0\}, \{\phi_1 \leq 0, \phi_2 = 0\}. \end{aligned}$$

Now, keeping u^{++}, u^{+-}, u^{-+}, u^{--} fixed, as C^1 functions on their corresponding domains up to all boundary points, we can formally write the Euler-Lagrange equations associated with the minimization problem with respect to

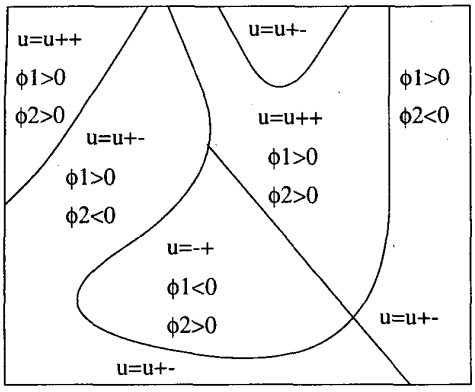

Figure 6. Example of partition of the image u in regions, with the boundaries Γ represented via two level set functions ($\phi_1 = 0, \phi_2 = 0$), and with smooth value-functions u^{++}, u^{+-}, u^{-+} and u^{--}, on each side of the curves making up Γ.

ϕ_1 and ϕ_2, after regularization of H:

$$\frac{\partial \phi_1}{\partial t} = \delta_\varepsilon(\phi_1)\Big[\nu\nabla\Big(\frac{\nabla\phi_1}{|\nabla\phi_1|}\Big) - |u^{++} - u_0|^2 H(\phi_2) - \mu|\nabla u^{++}|^2 H(\phi_2) - |u^{+-} - u_0|^2(1 - H(\phi_2)) - \mu|\nabla u^{+-}|^2(1 - H(\phi_2)) + |u^{-+} - u_0|^2 H(\phi_2) + \mu|\nabla u^{-+}|^2 H(\phi_2) + |u^{--} - u_0|^2(1 - H(\phi_2)) + \mu|\nabla u^{--}|^2(1 - H(\phi_2))\Big] = 0,$$

and

$$\frac{\partial \phi_2}{\partial t} = \delta_\varepsilon(\phi_2)\Big[\nu\nabla\Big(\frac{\nabla\phi_2}{|\nabla\phi_2|}\Big) - |u^{++} - u_0|^2 H(\phi_1) - \mu|\nabla u^{++}|^2 H(\phi_1) + |u^{+-} - u_0|^2 H(\phi_1) + \mu|\nabla u^{+-}|^2 H(\phi_1) - |u^{-+} - u_0|^2(1 - H(\phi_1)) - \mu|\nabla u^{-+}|^2(1 - H(\phi_1)) + |u^{--} - u_0|^2(1 - H(\phi_1)) + \mu|\nabla u^{--}|^2(1 - H(\phi_1))\Big].$$

Finally, we show in Figure 8 numerical results on a real noisy image (shown in Figure 7), using this four-phase model. We show the evolution of the curves, superposed over the initial noisy image u_0, together with the denoised versions of u, at different increasing times. At the initial time, the two curves given by $\{\phi_1 = 0\}$ and $\{\phi_2 = 0\}$ are shown in different colors (we use here the so-called seed initialization).

It is well known that, by minimizing the Mumford-Shah energy, steep gradients and artificial edges can be introduced. This can be seen in the numerical results in Figure 8. On the other hand, the Mumford-Shah model has other limitations, by allowing only for triple junctions with 120^o, and that edges meeting the boundary, need to be perpendicular on it. This restrictions on the type of edges are due to the length term. In the model presented in this subsection, we have slightly changed this edge-term, in order to have less complicated equations in ϕ_1 and ϕ_2. By this change, other types of edges and junctions are allowed.

We have mentioned in the introduction existence results for the Mumford-Shah minimization problem (but the global minimizer is not unique). We can also show, by standard techniques of the calculus of variations on the space $SBV(\Omega)$ (special functions of bounded variations), and a compactness result due to L. Ambrosio [1], that the proposed minimization problems from this paper, in the level set formulation, have a minimizer. Finally, because there is no uniqueness of the minimizers, and because the problems are non-convex, the numerical results may depend on the initial choice of the curves, and we may compute a local minimum only. We think that, using the seed initialization, the algorithms have the tendency of computing a global minimum.

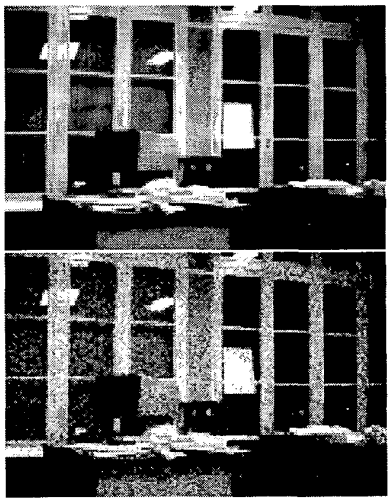

Figure 7. Original and noisy image.

3. Concluding remarks

We have proposed in this paper a level set algorithm for the general Mumford-Shah segmentation problem. This is a functional with free boundaries and jumps. We have shown that, in two dimensions, two level set functions suffice to represent any piecewise-smooth function, and our main idea is based on the Four Color Theorem.

Figure 8. Curves over u_0 and denoised u for increasing times, by the 4-phase model.

We have presented numerical results using the proposed algorithm. Finally, we can view the presented level set formulation for the Mumford-Shah problem as a common framework for active contours, segmentation, denoising and edge-detection.

Acknowledgments

The authors would like to thank the unknown reviewers for their useful remarks and suggestions, and also Paul Burchard, Ronald Fedkiw, Riccardo March, and Stanley Osher, for very fruitful discussions.

Appendix: description of the algorithm

We give here the principal steps of the numerical algorithm for solving the Euler-Lagrange equations (3)-(4)-(5) from subsection 2.2. The other Euler-Lagrange equations are solved in a similar way.

We use standard finite differences discretizations of the equations, and similar implicit numerical scheme used in [12], applied to (5), and we construct the sequences of functions ϕ^n, $(u^+)^n$ and $(u^-)^n$, with $n \geq 0$, as follows:

1. Let $n = 0$; define the initial level set function ϕ^0.
2. Find $(u^+)^n$ on $\phi^n \geq 0$ and $(u^-)^n$ on $\phi^n \leq 0$ by (3-4).
3. Extend by C^1 functions $(u^+)^n$ on $\phi^n < 0$ and $(u^-)^n$ on $\phi^n > 0$ (near the curve).
4. Solve (5) to obtain ϕ^{n+1}.
5. Re-initialization of ϕ^n to the signed distance function to the curve, performed only locally, near the zero level set (for more details on re-initialization to the distance function, see [32]).

Step 3 is necessarily because, in order to solve in practice (5), we work on a narrow band around $\{\phi = 0\}$, but u^+ is not defined on $\{\phi < 0\}$ and u^- is not defined on $\{\phi > 0\}$.

To extend u^+ on $\{\phi < 0\}$ and u^- on $\{\phi > 0\}$ (at least near the curve), we have considered several possibilities. Let us denote by $\vec{N} = \frac{\nabla\phi}{|\nabla\phi|}$, the normal to the zero-level curves of ϕ.

For example, to obtain a C^1 extension of u^- on $\phi > 0$, we can solve to the steady state the following degenerate elliptic linear equation: $u_t^- = \nabla^2 u^-(\vec{N}, \vec{N})$ on $\phi > 0$, with the boundary condition $\partial u^-/\partial\vec{n} = 0$ on $\partial\Omega$. The right-hand-side of the above equation is the second order derivative of u^- in the normal direction $\vec{N}$.

A second possibility is by the "Ghost Fluid Method", first used in [13], then in [18], [17]: for example, for a C^0 extension of u^- to $\phi > 0$, solve to the steady state: $u_t^- + \vec{N} \cdot \nabla u^- = 0$ in $\{\phi > 0\}$. We can obtain higher order interpolations, applying the same method to $u_{\vec{N}}^- = \vec{N} \cdot \nabla u^-$ (to obtain a C^1 interpolation in the normal direction), etc.

A third possibility is by using minimal Lipschitz extensions [19], [6]. The idea is, in order to extend u^- in the region $\phi > 0$, solve $\nabla^2 u^-(\nabla u^-, \nabla u^-) = 0$.

References

[1] L. Ambrosio. A compactness theorem for a special class of functions of bounded variation. *Boll. Un. Mat. It.*, 3(B):857–881, 1989.

[2] L. Ambrosio and V. M. Tortorelli. Approximation of functionals depending on jumps by elliptic functionals via Gamma-convergence. *Comm. Pure Appl. Math.*, (43):999–1036, 1990.

[3] L. Ambrosio and V. M. Tortorelli. On the approximation of free discontinuity problems. *Boll. U.M.I.*, 6-B(7):105–123, 1992.

[4] B. Bourdin. Image segmentation with a finite element method. *M2AN Math. Model. Numer. Anal.*, 33(2):229–244, 1999.

[5] B. Bourdin and A. Chambolle. Implementation of a finite-elements approximation of the Mumford-Shah functional. *Numer. Math.*, 85(4):609–646, 2000.

[6] V. Caselles, J.-M. Morel, and C. Sbert. An Axiomatic Approach to Image Interpolation. *IEEE Transactions on Image Processing*, 7(3):376–386, 1998.

[7] A. Chambolle. Image segmentation by variational methods: Mumford and Shah functional and the discrete approximations. *SIAM J. Appl. Math.*, 55(3):827–863, 1995.

[8] A. Chambolle. Finite-differences discretizations of the Mumford-Shah functional. *M2AN Math. Model. Numer. Anal.*, 33(2):261–288, 1999.

[9] A. Chambolle and G. D. Maso. Discrete approximation of the Mumford-Shah functional in dimension two. *M2AN Math. Model. Numer. Anal.*, 33(4):651–672, 1999.

[10] T. Chan, B. Y. Sandberg, and L. Vese. Active Contours without Edges for Vector-Valued Images. *J. of Visual Communication and Image Representation*, (11):130–141, 2000.

[11] T. Chan and L. Vese. Image segmentation using level sets and the piecewise-constant Mumford-Shah model. *UCLA CAM Report 00-14, submitted to IJCV*, 2000.

[12] T. Chan and L. Vese. Active Contours Without Edges. *IEEE Transactions on Image Processing*, 10(2):266–277, 2001.

[13] S. Chen, B. Merriman, S. Osher, and P. Smereka. A simple level set method for solving Stefan problems. *J. Comput. Physics*, (0135):8–29, 1997.

[14] G. Dal Maso, J.-M. Morel, and S. Solimini. A variational method in image segmentation: existence and approximation results. *Acta Matematica*, (168):89–151, 1992.

[15] S.-I. Ei, R. Ikota, and M. Mimura. Segregating partition problem in competition-diffusion systems. *Interfaces and Free Boundaries*, 1(1), 1999.

[16] L. Evans and R. Gariepy. *Measure Theory and Fine Properties of Functions*. CRC Press, 1992.

[17] R. P. Fedkiw. The Ghost Fluid Method for Numerical Treatment of Discontinuities and Interfaces. *UCLA CAM Report 99-31*, 1999.

[18] R. P. Fedkiw, T. Aslam, B. Merriman, and S. Osher. A non-oscillatory Eulerian approach to interfaces in multimaterial flows (the ghost fluid method). *Journal of Computational Physics*, 152(2):457–492, 1999.

[19] R. Jensen. Uniqueness of Lipschitz Extensions: Minimizing the Sup Norm of the Gradient. *Arch. Rat. Mech. Anal.*, (123):51–74, 1993.

[20] G. Koepfler, C. Lopez, and J.-M. Morel. A multiscale algorithm for image segmentation by variational method. *SIAM J. of Num. Anal.*, 31(1):282–299, 1994.

[21] R. March. Visual reconstruction with discontinuities using variational methods. *Image and Vision Computing*, (10):30–38, 1992.

[22] J.-M. Morel and S. Solimini. Segmentation of images by variational methods: a constructive approach. *Revista Matematica Universidad Complutense de Madrid*, (1):169–182, 1988.

[23] J.-M. Morel and S. Solimini. Segmentation d'images par méthode variationnelle: une preuve constructive d'existence. *C.R. Acad. Sci. Paris Série I, Math.*, (308):465–470, 1989.

[24] J.-M. Morel and S. Solimini. *Variational Methods in Image Segmentation*. Birkhauser, PNLDE 14, 1994.

[25] D. Mumford and J. Shah. Optimal approximation by piecewise smooth functions and associated variational problems. *Comm. Pure Appl. Math.*, (42):577–685, 1989.

[26] S. Osher and J. A. Sethian. Fronts Propagating with Curvature-Dependent Speed: Algorithms Based on Hamilton-Jacobi Formulation. *Journal of Computational Physics*, (79):12–49, 1988.

[27] N. Paragios and R. Deriche. Coupled geodesic active regions for image segmentation: a level set approach. *Proc. 6th European Conference on Computer Vision, Dublin*, (2):224–240, 2000.

[28] C. Samson, L. Blanc-Féraud, G. Aubert, and J. Zerubia. A level set model for image classification. *International Journal of Computer Vision*, 40(3):187–197, 2000.

[29] J. Shah. A Common Framework for Curve Evolution, Segmentation and Anisotropic Diffusion. *IEEE Conference on Computer Vision and Pattern Recognition*, 1996.

[30] J. Shah. Riemannian Drums, Anisotropic Curve Evolution and Segmentation. *Scale-Space Theories in Computer Vision, Proc. Second Int. Conf. Scale-Space'99, LNCS*, (1682), 1999.

[31] J. B. Shi and J. Malik. Normalized cuts and image segmentation. *IEEE Transactions on PAMI*, 22(8):888–905, 2000.

[32] M. Sussman, P. Smereka, and S. Osher. A level set approach for computing solutions to incompressible two-phase flow. *J. Comput. Phys.*, 119:146–159, 1994.

[33] A. Tsai, A. Yezzi, and A. S. Willsky. A Curve Evolution Approach to Medical Image Magnification via the Mumford-Shah Functional. *MICCAI*, pages 246–255, 2000.

[34] A. Yezzi, A. Tsai, and A. Willsky. A statistical approach to snakes for bimodal and trimodal imagery. *Int. Conf. on Computer Vision*, 1999.

[35] H. K. Zhao, T. Chan, B. Merriman, and S. Osher. A Variational Level Set Approach to Multiphase Motion. *J. Comput. Phys.*, (127):179–195, 1996.

[36] S. C. Zhu, T. S. Lee, and A. L. Yuille. Region competition: Unifying snakes, region growing, energy/Bayes/MDL for multi-band image segmentation. *Proc. IEEE 5th ICCV, Cambridge*, pages 416–423, 1995.